Warfare: Breaking the Watermark Protection of AI-Generated Content

Guanlin Li^{1,2}, Yifei Chen³, Jie Zhang¹, Jiwei Li^{4,5}, Shangwei Guo³, Tianwei Zhang¹

¹Nanyang Technological University, ²S-Lab, NTU,

³Chongqing University, ⁴Shannon.AI, ⁵Zhejiang University.

quanlin001@e.ntu.edu.sq

Abstract

AI-Generated Content (AIGC) is gaining great popularity, with many emerging commercial services and applications. These services leverage advanced generative models, such as latent diffusion models and large language models, to generate creative content (e.g., realistic images and fluent sentences) for users. The usage of such generated content needs to be highly regulated, as the service providers need to ensure the users do not violate the usage policies (e.g., abuse for commercialization, generating and distributing unsafe content). A promising solution to achieve this goal is watermarking, which adds unique and imperceptible watermarks on the content for service verification and attribution. Numerous watermarking approaches have been proposed recently. However, in this paper, we show that an adversary can easily break these watermarking mechanisms. Specifically, we consider two possible attacks. (1) Watermark removal: the adversary can easily erase the embedded watermark from the generated content and then use it freely bypassing the regulation of the service provider. (2) Watermark forging: the adversary can create illegal content with forged watermarks from another user, causing the service provider to make wrong attributions. We propose Warfare, a unified methodology to achieve both attacks in a holistic way. The key idea is to leverage a pre-trained diffusion model for content processing and a generative adversarial network for watermark removal or forging. We evaluate Warfare on different datasets and embedding setups. The results prove that it can achieve high success rates while maintaining the quality of the generated content. Compared to existing diffusion model-based attacks, Warfare is $5,050 \sim 11,000 \times$ faster.

1. Introduction

Benefiting from the advance of generative deep learning models [40, 43], AI-Generated Content (AIGC) has become increasingly prominent. Many commercial services have been released, which leverage large models (e.g., Chat-

GPT [9], Midjourney [4]) to generate creative content based on users' demands. The rise of AIGC also leads to some legal considerations, and the service provider needs to set up some policies to regulate the usage of generated content. *First*, the generated content is one important intellectual property of the service provider. Many services do not allow users to make it into commercial use [4, 43]. Selling the generated content for financial profit [5] will violate this policy and cause legal issues. *Second*, generative models have the potential of outputting unsafe content [29, 33, 38, 46], such as fake news [18], malicious AI-powered images [29, 41], phishing campaigns [19], and cyberattack payloads [12]. New laws are established to regulate the generation and distribution of content from deep learning models on the Internet [1, 2, 6].

As protecting and regulating AIGC become urgent, Google hosted a workshop in June 2023 to discuss the possible solutions against malicious usage of generative models [11]. Not surprisingly, the watermarking technology is mentioned as a promising defense. By adding invisible specific watermark messages to the generated content [17, 27, 34], the service provider is able to identify the misuse of AIGC and track the corresponding users. A variety of robust watermarking methodologies have been designed, which can be classified into two categories. (1) A general strategy is to make the generative model learn a specific data distribution, which can be decoded by another deep learning model to obtain a secret message as the watermark [17, 34, 53]. (2) The service provider can concatenate a watermark embedding model [42, 55] after the generative model to make the final output contain watermarks. A very recent work from DeepMind, SynthID Beta [7], detects AIgenerated images by adding watermarks to the generated images¹. According to its description, this service possibly follows a similar strategy as StegaStamp [42], which adopts an encoder to embed watermarks into images and a decoder to identify the embedded watermarks in the given images.

The Google workshop [11] reached the consensus that

¹Up to the date of writing, SynthID Beta is still a beta product only provided to a small group of users. Since we do not have access to it, we do not include evaluation results with respect to it in our experiments.

"existing watermarking algorithms only withstand attacks when the adversary has no access to the detection algorithm", and embedding a watermark to a clean image or text "seems harder for the attacker, especially if the watermarking process involves a secret key". However, in this paper, we argue that it is not the case. We find that it is easy for an adversarv without any prior knowledge to **remove** or **forge** the embedded secret watermark in AIGC, which will break the IP protection and content regulation. Specifically, (1) a watermark removal attack makes the service providers fail to detect the watermarks which are embedded into the AIGC previously, so the malicious user can circumvent the policy regulation and abuse the content for any purpose. (2) A watermark forging attack can intentionally embed the watermark of a different user into the unsafe content without the knowledge of the secret key. This could lead to wrong attributions and frame up that benign user.

Researchers have proposed several methods to achieve watermark removal attacks [30, 31, 36, 44, 45, 52]. However, they suffer from several limitations. For instance, some attacks require the knowledge of clean data [31, 44] or details of watermarking schemes [36, 45], which are not realistic in practice. Some attacks take extremely long time to remove the watermark from one image [30, 52]. Besides, there are currently no studies towards watermark forging attacks. More detailed analysis can be found in Section 2.2.

To remedy the above issues, we introduce Warfare, a novel and efficient methodology to achieve both watermark forge and removal attacks against AIGC in a unified manner. The key idea is to leverage a pre-trained diffusion model and train a generative adversarial network (GAN) for erasing or embedding watermarks to AIGC. Specifically, the adversary only needs to collect the watermarked AIGC from the target service or a specific user, without any clean content. Then he can adopt a public diffusion model, such as DDPM [22], to denoise the collected data. The preprocessing operation of the diffusion model can make the embedded message unrecoverable from the denoised data. Finally, the adversary trains a GAN model to map the data distribution from collected data to denoised data (for watermark removal) or from denoised data to collected data (for watermark forge). After this model is trained, the adversary can adopt the generator to remove or forge the specific watermark for AIGC.

We evaluate our proposed Warfare on various datasets (e.g., CIFAR-10, CelebA), and settings (e.g., different watermark lengths, few-shot learning), to show its generalizability. Our results prove that the adversary can successfully remove or forge a specific watermark in the AIGC and keep the content indistinguishable from the original one. This provides concrete evidence that existing watermarking schemes are not reliable, and the community needs to explore more robust watermarking methods. Overall, our contribution can be summarized as follows:

- To the best of our knowledge, it is the first work focusing on removing and forging watermarks in AIGC under a black-box threat model. Furthermore, Warfare is a unified methodology, which can achieve both attack goals in a holistic way. Our study discloses the unreliability and fragility of existing watermarking schemes.
- Different from prior attacks, Warfare does not require the adversary to have clean data or any information about the watermarking schemes, which is more practical in real-world applications.
- Comprehensive evaluation proves that Warfare can remove or forge the watermarks without harming the data quality. It is **time-efficient**, which is 5,050~11,000× faster than existing attacks based on diffusion models.
- Warfare is effective in the few-shot setting, i.e., it can be **freely adapted to unseen watermarks**. Furthermore, it remains highly effective for different watermark lengths.

2. Related Works

2.1. Content Watermark

Driven by the rapid development of large and multi-modal models, there is a renewed interest in generative models, such as ChatGPT [9] and Stable Diffusion [40], due to their capability of creating high-quality images [22, 40], texts [9, 43], audios [28], and videos [23]. Such AI-Generated Content (AIGC) can have high IP values and sensitive information. Therefore, it is important to protect and regulate it during its distribution on public platforms, e.g., Twitter [8] and Instagram [3].

A typical strategy to achieve the above goal is watermarking: the service provider adds a secret and unique message to the content, which can be subsequently extracted for ownership verification and attribution. Existing watermarking schemes can be divided into post hoc methods and prior methods. Post hoc methods convert the clean content into watermarked content using one of the following two strategies. (i) Visible watermark strategy: the service provider adds characters or paintings into the clean content [13, 32, 47], which can be recognized by humans. (ii) Invisible watermark strategy: the service provider embeds a specific bit string into the clean content by a pre-trained steganography model [42, 55] or signal transformation [36], which will be decoded by a verification algorithm later.

For prior methods, the generative model directly learns a distribution of watermarked content, which can be decoded by a verification algorithm [14, 15, 17, 53]. Specifically, Fei et al. [15] designed a watermarking scheme for generative adversarial networks (GANs), by learning the distribution of watermarked images supervised by the watermark decoder. A watermarking scheme [17, 53] is designed for diffusion models [40], which embeds a predefined bit string into the generated images, and later uses a secret decoder to extract

it. The service provider can recognize the AIGC from his generative model or determine the specific user account.

2.2. Watermark Attacks

To the best of our knowledge, there is no work considering the watermark forging attack. Prior efforts mainly focus on the watermark removal attack. These attack solutions can be summarized into three main categories, i.e., image inpainting methods [31, 44] for visible watermarks, denoising methods [30, 52], and disrupting methods [36, 45] for invisible watermarks. However, they have several critical drawbacks in practice. Specifically, the image inpainting methods [31, 44] require clean images and watermarked images to train the inpainting model, which is not feasible in the real world, because the user can only obtain watermarked images from the service providers [4]. Disrupting methods [36, 45] require the user to know the details of the watermarking schemes, which is also difficult to achieve. The most promising method is based on denoising models. For instance, [30] adopted guided diffusion models to purify the watermarked images and minimize the differences between the watermarked images and diffusion model's outputs. However, using diffusion models to remove the watermark will cost a lot of time. Our proposed Warfare aims to address all of these limitations.

3. Preliminary

3.1. Scope

In this paper, we target both post hoc and prior watermarking methods. For post hoc methods, we do not consider visible watermarks as they can significantly decrease the visual quality of AIGC, making them less popular for practical adoption. For instance, the Tree-Ring watermark [47] is proven to significantly change both pixel and latent spaces [52], which is treated as "a visible watermark". Hence, it is beyond the scope of this paper. For invisible watermarks, we only consider the steganography approach, as it is much more robust and harder to attack than the signal transformation approach [36, 45, 52]. We mainly consider watermarks embedded in the generated images. Watermarks in other other domains, e.g., language, audio, will be our future work.

3.2. Watermark Verification Scheme

We consider the most popular type of secret message used in watermarking implementations: bit strings [14, 15, 17, 53]. When a service provider P employs a generative model \mathcal{M}_G to generate creative images for public users, P employs a watermarking scheme (e.g., [17, 34]) to embed a secret userspecific bit string m of length L in each generated image. To verify whether a suspicious image x^s is watermarked by P for a specific user, P uses a pre-trained decoder \mathcal{M}_D to extract the bit string m^s from x^s . Then, P calculates the

Hamming Distance between m and m^s : $\mathrm{HD}(m,m^s)$. If $\mathrm{HD}(m,m^s) \leq (1-\tau)L$, where τ is a pre-defined threshold, P will believe that x^s contains the secret watermark m.

3.3. Threat Model

Attack Goals. A malicious user can break this watermarking scheme with two distinct goals. (1) Watermark removal attack: the adversary receives a generated image from the service provider, which contains the secret watermark associated with him. He aims to erase the watermark from the generated image, and then use it freely without the constraint of the service policy, as the provider is not able to identify the watermarks and track him anymore. (2) Watermark forging attack: the adversary tries to frame up a victim user by forging the victim's watermark on a malicious image (from another model or created by humans). Then the adversary can distribute the image on the Internet. The service provider will attribute to the wrong user.

Adversary's capability. We consider the black-box scenario, where the adversary can only obtain the generated image and has no knowledge of the employed generative model or watermark scheme. This is practical, as many service providers only release APIs for users to use their models without leaking any information about the details of the backend models \mathcal{M}_G and \mathcal{M}_D . We further assume that all the generated images from the target service are watermark-protected, so the adversary cannot collect any clean images. These assumptions increase the attack difficulty compared to prior works [31, 36, 44, 45].

4. Warfare: A Unified Attack Methodology

We introduce Warfare to manipulate watermarks with the above goals. Let x_i denote a clean image, and x_i' denote the corresponding watermarked image. These two images are visually indistinguishable. Our goal is to establish a bidirectional mapping $x_i \longleftrightarrow x_i'$. For the watermark removal attack, we can derive x_i from x_i' . For the watermark forging attack, we can construct x_i' from x_i .

However, it is challenging for the adversary to identify the relationship between x_i and x_i' , as he has no access to the clean image x_i . To address this issue, the adversary can adopt a pre-trained denoising model to convert x_i' into a mediator image $\hat{x_i}$. Due to the denoising operation, $\hat{x_i}$ is visually different from x_i , but does not contain the watermark. Therefore, it will follow a similar "non-watermarked" distribution as x_i . Then the adversary can train a GAN model between x_i and x_i' , which is guided by $\hat{x_i}$. Figure 1 shows the overview of Warfare, which consists of three steps. Below, we describe the details.

4.1. Data Collection

The adversary collects a set of images x_i' generated by the target service provider for one user. All the collected data

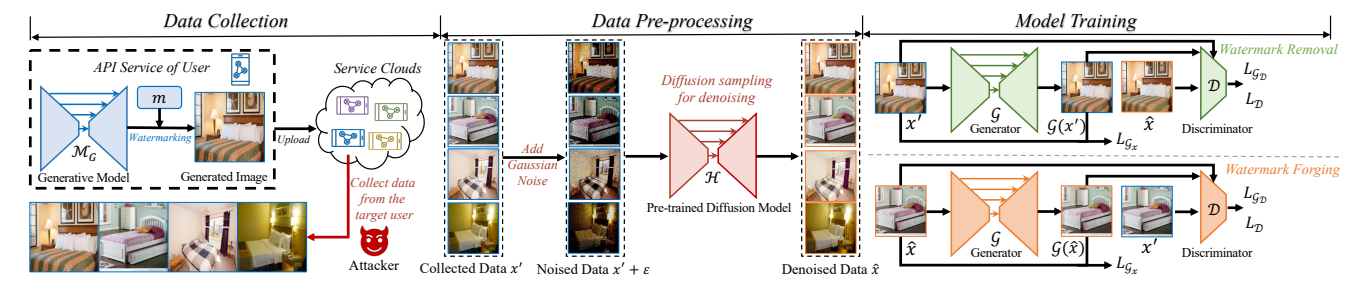


Figure 1. Overview of Warfare. (1) Collecting watermarked data from the target AIGC service or Internet. (2) Using a public pre-trained denoising model to purify the watermarked data. (3) Adopting the watermarked and mediator data to train a GAN, which can be used to remove or forge the watermark. x' is the watermarked image. \hat{x} is the mediator image. The subscript i is omitted.

contain one specific watermark m associated with this user. For the watermark removal attack, the adversary can query the service to collect the watermarked images with his own account, from which he aims to remove the watermark. For the watermark forging attack, the adversary can possibly collect such data from the victim user's social account. This is feasible as people enjoy sharing their created content on the Internet and adding tags to indicate the used service. Then the adversary can forge the watermark of the victim user on any images to cause wrong attribution. In either case, a dataset $\mathcal{X}' = \{x_i' | x_i' \sim (\mathcal{M}_G, m)\}$ is established, where \mathcal{M}_G is the service provider's generative model.

4.2. Data Pre-processing

Given the collected watermarked dataset \mathcal{X}' , since the adversary does not have the corresponding non-watermarked dataset X, he cannot directly build the mapping. Instead, he can adopt a public pre-trained denoising model \mathcal{H} to preprocess \mathcal{X}' and obtain the corresponding mediator dataset $\hat{\mathcal{X}}$. The goal of the denoising model is to remove the watermark m from \mathcal{X}' . Since existing watermarking schemes are designed to be very robust, we have to increase the denoising strength significantly, in order to distort the embedded watermark. Therefore, we first add very large-scale noise ϵ_i into x_i' and then apply a diffusion model \mathcal{H} to denoise the images, i.e., $\hat{\mathcal{X}} = {\hat{x}_i | \mathcal{H}(x_i' + \epsilon_i) = \hat{x}_i, x_i' \in \mathcal{X}', \epsilon_i \in \mathcal{N}(\mathbf{0}, \mathbf{I})}.$ This will make \hat{x}_i highly visually different from x'_i and x_i . Figure 2 shows some visualization results of x_i' and \hat{x}_i , and we can observe that they keep some similar semantic information but look very different. Table 3 proves that \hat{x}_i does not contain any watermark information due to the injected large noise and strong denoising operation.

The mediator dataset $\hat{\mathcal{X}}$ can be seen as being drawn from the same "non-watermarked" distribution as \mathcal{X} , which is different from \mathcal{X}' of the "watermarked" distribution. Therefore, it can help discriminate watermarking images from non-watermarked images and build connections between them. This is achieved in the next step, as detailed below.

4.3. Model Training

With the watermarked data x' and non-watermarked data \hat{x} , the adversary can train a GAN model to add or remove

watermarks. This GAN model consists of a generator \mathcal{G} and a discriminator \mathcal{D} : \mathcal{G} is used to generate x from x' (watermark removal) or generate x' from x (watermark forging); \mathcal{D} is used to discriminate whether the input is drawn from the distribution of watermarked images x' or the distribution of non-watermarked images \hat{x} . Below, we describe these two attacks, separately.

Watermark removal attack. In this attack, the generator \mathcal{G} is built to obtain x from x', i.e., $x = \mathcal{G}(x')$, where x' and x should be visually indistinguishable. x generated by \mathcal{G} should make \mathcal{D} believe it is from the same nonwatermarked image distribution as \hat{x} , because x should be a non-watermarked image. Meanwhile, \mathcal{D} should recognize x as a watermarked image, since it is very close to x'. Therefore, the loss functions $L_{\mathcal{G}}$ for \mathcal{G} and $L_{\mathcal{D}}$ for \mathcal{D} are:

$$\begin{split} L_{\mathcal{D}} &= -\mathbb{E}_{\hat{x} \in \hat{\mathcal{X}}} \mathcal{D}(\hat{x}) + \mathbb{E}_{x' \in \mathcal{X}'} \mathcal{D}(\mathcal{G}(x')) \\ &+ w_{\mathcal{D}} \mathbb{E}_{\hat{x} \in \hat{\mathcal{X}}, x' \in \mathcal{X}'} \nabla_{\alpha x' + (1-\alpha)\hat{x}} \mathcal{D}(\alpha x' + (1-\alpha)\hat{x}), \\ L_{\mathcal{G}_{D}} &= -w_{\mathcal{G}} \mathbb{E}_{x' \in \mathcal{X}'} \mathcal{D}(\mathcal{G}(x')), \\ L_{\mathcal{G}_{x}} &= \mathbb{E}_{x' \in \mathcal{X}'} [\mathrm{L}_{1}(\mathcal{G}(x'), x') + \mathrm{MSE}(\mathcal{G}(x'), x') \\ &+ \mathrm{LPIPS}(\mathcal{G}(x'), x')], \\ L_{\mathcal{G}} &= L_{\mathcal{G}_{D}} + w_{x} L_{\mathcal{G}_{x}}, \end{split}$$

where w_D , w_G , and w_x are the weights for losses and α is a random variable between 0 and 1 [10]². L₁ is the L_1 -norm, MSE is the mean squared error loss, and LPIPS is the perceptual loss [51]. They can guarantee the quality of the generated image x.

Watermark forging attack. In this attack, the generator \mathcal{G} is built to obtain \hat{x}' from \hat{x} , i.e., $\hat{x}' = \mathcal{G}(\hat{x})$, where \hat{x}' and \hat{x} should be visually indistinguishable. \hat{x}' is the watermarked version of \hat{x} . \hat{x}' generated by \mathcal{G} should make \mathcal{D} believe it is from the same watermarked image distribution as x', because \hat{x}' should be a watermarked image. But \mathcal{D} should recognize \hat{x}' as a non-watermarked image, since it is very close to \hat{x} . Therefore, the loss functions $L_{\mathcal{G}}$ for \mathcal{G} and $L_{\mathcal{D}}$

²We slightly modify the discriminator loss for large-resolution images to stabilize the training process. Details are in the supplementary materials.

Bit Length		Original					Watermark Remove					Wat	ermark Fo	orge	ge			
	Bit Acc	FID	PSNR	SSIM	CLIP	Bit Acc↓	FID↓	PSNR↑	SSIM↑	CLIP↑	Bit Acc ↑	FID↓	PSNR↑	SSIM↑	CLIP ↑			
4 bit	100.00%	4.22	27.81	0.89	0.99	52.53%	16.36	24.51	0.86	0.92	95.76%	17.59	26.70	0.88	0.94			
8 bit	100.00%	6.19	25.23	0.83	0.99	47.80%	18.42	23.59	0.83	0.91	97.84%	21.09	24.94	0.82	0.93			
16 bit	100.00%	11.34	22.71	0.73	0.98	50.10%	24.63	23.44	0.77	0.91	92.23%	18.34	25.84	0.83	0.94			
32 bit	99.99%	28.76	19.99	0.53	0.96	53.64%	25.33	21.17	0.64	0.91	90.14%	31.13	23.41	0.71	0.93			

Table 1. Performance of Warfare under different bit lengths on CIFAR-10. The number of images for the adversary is 25,000. ↓ means lower is better. ↑ means higher is better.

# of Samples		Original					Watermark Remove					Watermark Forge			
(bit length = 8bit)	Bit Acc	FID	PSNR	SSIM	CLIP	Bit Acc↓	FID↓	PSNR↑	SSIM↑	CLIP↑	Bit Acc ↑	FID↓	PSNR↑	SSIM↑	CLIP↑
5000						49.42%	20.75	24.64	0.83	0.92	96.11%	18.86	24.36	0.83	0.93
10000						50.68%	23.76	24.31	0.82	0.90	98.63%	15.68	24.70	0.81	0.94
15000	100.00%	6.19	25.23	0.83	0.99	59.88%	20.32	22.87	0.80	0.92	97.80%	25.34	24.55	0.80	0.92
20000						54.59%	22.90	24.93	0.84	0.90	95.99%	23.56	23.74	0.80	0.92
25000						47.80%	18.42	23.59	0.83	0.91	97.84%	21.09	24.94	0.82	0.93

Table 2. Performance of Warfare under the different number of collected images on CIFAR-10. The length of embedded bits is 8.

for \mathcal{D} are:

$$L_{\mathcal{D}} = -\mathbb{E}_{x'\in\mathcal{X}'}\mathcal{D}(x') + \mathbb{E}_{\hat{x}\in\hat{\mathcal{X}}}\mathcal{D}(\mathcal{G}(\hat{x}))$$

$$+ w_{\mathcal{D}}\mathbb{E}_{\hat{x}\in\hat{\mathcal{X}},x'\in\mathcal{X}'}\nabla_{\alpha x'+(1-\alpha)\hat{x}}\mathcal{D}(\alpha x'+(1-\alpha)\hat{x}),$$

$$L_{\mathcal{G}_{D}} = -w_{\mathcal{G}}\mathbb{E}_{\hat{x}\in\hat{\mathcal{X}}}\mathcal{D}(\mathcal{G}(\hat{x})),$$

$$L_{\mathcal{G}_{x}} = \mathbb{E}_{\hat{x}\in\hat{\mathcal{X}}}[L_{1}(\mathcal{G}(\hat{x}),\hat{x}) + \mathrm{MSE}(\mathcal{G}(\hat{x}),\hat{x}) + \mathrm{LPIPS}(\mathcal{G}(\hat{x}),\hat{x})],$$

$$L_{\mathcal{G}} = L_{\mathcal{G}_{D}} + w_{x}L_{\mathcal{G}_{x}}.$$

The notations are the same as these in the watermark removal attack. It is easy to find that for both types of attacks, the training framework can be seen as a *unified* one, because the adversary only needs to replace x' with \hat{x} or replace \hat{x} with x', to switch to another attack.

5. Evaluations

5.1. Experiment Setup

Datasets. We mainly consider two datasets: CIFAR-10 and CelebA [35]. CIFAR-10 contains 50,000 training images and 10,000 test images with a resolution of 32*32. CelebA is a celebrity faces dataset, which contains 162,770 images for training and 19,867 for testing, resized at a resolution of 64*64 in our experiments. We randomly split the CIFAR-10 training set into two disjoint parts, one of which is to train the service provider's model and another is used by the adversary. Similarly, we randomly pick 100,000 images for the service provider and 10,000 images for the adversary from the CelebA training set. Furthermore, we also consider a more complex dataset with high resolution, LSUN [49]. Details can be found in the supplementary materials.

Watermarking Schemes. Considering the watermark's expandability to multiple users, we mainly adopt the post hoc manner, i.e., adding user-specific watermarks to the generated images. We adopt StegaStamp [42], a state-of-the-art and robust method for embedding bit strings into given images, which is proved to be the most effective watermarking embedding method against various removal attacks [52]. On the other hand, watermarking schemes, such as RivaGAN [50] and SSL [16], have been shown to be not

robust [52]. Therefore, we only consider breaking water-marking schemes, which have not been broken before. We also provide two case studies to explore the prior manner, which directly generates images with watermarks for our case studies. We follow previous works [15, 53] to embed a secret watermark to WGAN-div [48] and EDM [26].

Baselines. To the best of our knowledge, Warfare is the first work to remove or forge a watermark in images under a pure black-box threat model. Therefore, we consider some potential baseline attack methods under the same assumptions and attacker's capability, i.e., having only watermarked images. These baseline methods can be classified into two groups. (1) Image transformation methods: we consider modifying the properties of the given image, such as resolution, brightness, and contrast. We also consider image compression (e.g., JPEG) and image disruptions (e.g., Gaussian blurring, adding Gaussian noise). (2) Diffusion model methods [30]: we directly adopt a pre-trained unconditional diffusion model (DiffPure [37]) to modify the given image, which does not require to train a diffusion model from scratch and does not need clean images. As the diffusion model is not trained or fine-tuned for watermark removal or forge, for consistency, we do not adopt guided diffusion models or conditional diffusion models as [30] did. The results from pre-trained diffusion models are various on different datasets, which will be discussed in the supplementary materials. Specifically, for watermark removal, the watermarked images are inputs for the attacks; for watermark forge, the clean images are inputs for the attacks.

Implementation. We adopt DiffPure [37] as the diffusion model used in the second step of Warfare without any fine-tuning. The diffusion model used in DiffPure depends on the domain of watermarked images. For example, if the watermarked images are human faces from CelebA and FFHQ, we use a diffusion model trained on CelebA. As the adversary does not have any knowledge of the watermarking scheme, it is important to decide which checkpoint should be used in the attack. We provide a simple way to help the adversary select a checkpoint during the training process in

Methods			Original				Wate	rmark Re	move			Wat	ermark Fo	orge	
Methods	Bit Acc	FID	PSNR	SSIM	CLIP	Bit Acc↓	FID↓	PSNR↑	SSIM↑	CLIP↑	Bit Acc ↑	FID↓	PSNR↑	SSIM↑	CLIP↑
CenterCrop						59.89%	-	-	-	0.90	48.33%	-	-	-	0.93
GaussianNoise						99.92%	53.80	24.97	0.71	0.86	52.28%	47.07	28.64	0.75	0.89
GaussianBlur						100.00%	25.09	26.26	0.84	0.86	52.10%	21.18	28.17	0.88	0.89
JPEG						99.27%	17.42	28.40	0.89	0.89	52.19%	9.96	33.36	0.94	0.90
Brightness						100.00%	4.26	19.70	0.87	0.95	52.28%	0.39	21.16	0.91	0.98
Gamma	100.00%	4.25	30.7	0.94	0.96	100.00%	4.43	22.93	0.88	0.96	52.32%	0.26	25.71	0.93	0.99
Hue						99.99%	5.93	26.84	0.93	0.94	52.21%	1.60	32.06	0.98	0.97
Contrast						100.00%	4.26	24.28	0.85	0.95	52.33%	0.25	27.62	0.90	0.98
DM_s						67.82%	73.30	20.61	0.62	0.69	48.78%	68.91	20.89	0.64	0.70
DM_l						47.20%	82.38	15.76	0.34	0.67	45.96%	79.06	15.81	0.34	0.68
Warfare						51.98%	9.93	26.61	0.91	0.90	99.11%	8.75	24.92	0.90	0.92

Table 3. Results of different attacks on CelebA. The bit string length is 32 bits. Best results in Bold. Second best results with Underline.

the supplementary materials. More details can be found in the supplementary materials, including all hyperparameters and used bit strings.

Metrics. To fairly evaluate our proposed Warfare, we consider five metrics to measure its performance from different perspectives. To determine the quality of the watermark removal (forging) task, we adopt Bit Acc, which can be calculated as Bit $\mathrm{Acc}(m,m') = \frac{|m| - \mathrm{HD}(m,m')}{|m|} \times 100\%$, where $\mathrm{HD}(\cdot,\cdot)$ is the Hamming Distance. If Bit $\mathrm{Acc}(m,m')\geq \tau$, verification will pass. Otherwise, it will fail. In our experiments, $\tau = 80\%$. To evaluate the quality of the images generated by Warfare and the baselines, we adopt the Fréchet Inception Distance (FID) [21], the peak signal-tonoise ratio (PSNR) [24], and the structural similarity index (SSIM) [24]. Furthermore, we consider the semantic information inside the images, which is evaluated by CLIP [39]. For the FID, PSNR, SSIM, and CLIP scores, we compute the results between clean images and watermarked images for the watermarking scheme, and between clean images and images after removal or forge attacks. For watermark removal, a lower bit accuracy is better. For watermark forging, a higher bit accuracy is better. For all tasks, a higher PSNR, SSIM, and CLIP score is better. And a lower FID is better.

5.2. Ablation Study

In this section, we explore the generalizability of our proposed Warfare under the views of the length of the embedding bits and the number of collected images. In Table 1, we show the results of Warfare at different lengths of embedded bits. The results indicate that Warfare is robust for different secret message lengths. Specifically, when the length of the embedded bits increases, Warfare can still achieve good performance on watermark removing or forging and make the transferred images keep high quality and maintain semantic information. In Table 2, we present the results when the adversary uses the different numbers of collected images as his training data. The results indicate that even with limited data, the adversary can remove or forge a specific watermark without harming the image quality, which proves that our method can be a real-world threat. Therefore, our proposed Warfare has outstanding

flexibility and generalizability under a practical threat model. We further prove its extraordinary few-shot generalizability for unseen watermarks in Section 5.3.

5.3. Results on Post Hoc Manners

Here, we focus on post hoc manners, i.e., adding watermarks to AIGC with an embedding model. Because the post hoc watermarking scheme can freely change the embedding watermarks, we evaluate Warfare under few-shot learning to show the capability of adapting to unseen watermarks.

Results on CelebA. We consider two different lengths of the embedding bits, i.e., 32-bit and 48-bit. Furthermore, we do not consider the specific coding scheme, including the source coding and the channel coding. Tables 3 and 4 compare Warfare and the baseline methods on the watermark removal task and the watermark forging task, respectively. We notice that the watermark embedding method is robust against various image transformations. Using image transformations cannot simply remove or forge a specific watermark in the given images. For methods using diffusion models, we consider two settings, i.e., adding large noise to the input (DM_l) and adding small noise to the input (DM_s) . Especially, we use the same setting as DM_l in the second step of Warfare to generate images. Although diffusion models can easily remove the watermark from the given images under both settings, the generated images are visually different from the input images, causing a low PSNR, SSIM, and CLIP score. Furthermore, the FID indicates that the diffusion model will cause a distribution shift compared to the clean dataset. Nevertheless, we find that DM_l and DM_s can maintain high image quality while successfully removing watermarks on other datasets, which we discuss in the supplementary materials. The results make us reflect on the generalizability of diffusion models on different datasets and watermarking schemes. However, evaluating all accessible diffusion models on various datasets and watermarking schemes will take months. Therefore, we leave it as future work to deeply study the diffusion models in the watermarking removal task. On the other hand, forging a specific unknown watermark is non-trivial and impossible for both image transformation methods and diffusion models.

Methods		(Original				Wate	rmark Rei	nove			Wat	ermark Fo	orge	
Wiethous	Bit Acc	FID	PSNR	SSIM	CLIP	Bit Acc↓	FID↓	PSNR↑	SSIM↑	CLIP↑	Bit Acc↑	FID↓	PSNR↑	SSIM↑	CLIP↑
CenterCrop						60.53%	-	-	-	0.87	50.12%	-	-	-	0.93
GaussianNoise						99.72%	62.36	23.39	0.68	0.83	51.71%	47.18	28.64	0.75	0.89
GaussianBlur						100.00%	33.23	24.84	0.81	0.85	52.06%	21.18	28.17	0.88	0.89
JPEG						99.30%	28.94	25.87	0.85	0.85	51.74%	9.96	33.36	0.94	0.90
Brightness						100.00%	13.37	18.96	0.83	0.91	51.83%	0.39	21.16	0.91	0.98
Gamma	100.00%	13.59	27.13	0.90	0.93	100.00%	13.68	21.72	0.84	0.92	51.92%	0.26	25.71	0.93	0.99
Hue						99.87%	15.82	24.79	0.88	0.90	51.86%	1.60	32.06	0.98	0.97
Contrast						100.00%	13.66	22.84	0.82	0.91	51.85%	0.25	27.62	0.90	0.98
DM_{s}						71.54%	78.67	20.21	0.60	0.69	49.35%	69.09	20.92	0.64	0.71
DM_l						53.75%	82.94	15.67	0.33	0.67	50.99%	81.66	15.82	0.34	0.68
Warfare						54.36%	19.98	25.29	0.88	0.88	94.61%	12.14	23.04	0.87	0.90

Table 4. Results of different attacks on CelebA. The bit string length is 48 bits.

# of Samples	Original					Watermark Remove					Watermark Forge				
(bit length = 32bit)	Bit Acc	FID	PSNR	SSIM	CLIP	Bit Acc↓	FID↓	PSNR↑	SSIM↑	CLIP↑	Bit Acc↑	FID↓	PSNR↑	SSIM↑	CLIP↑
10						49.98%	46.90	23.19	0.81	0.83	72.64%	12.27	22.43	0.89	0.91
50	100.00%	4.14	30.69	0.94	0.96	53.31%	19.74	24.47	0.87	0.86	83.18%	11.89	28.37	0.94	0.93
100						53.27%	14.30	25.51	0.89	0.87	93.47%	12.43	26.57	0.92	0.91

Table 5. Few-shot generalization ability of Warfare on unseen watermarks on CelebA.

Our Warfare gives an outstanding performance in both tasks and maintains good image quality as well. However, we notice that as the length of the embedded bit string increases, it becomes more challenging to forge or remove the watermark. That is the reason that under 48-bit length, our Warfare has a little performance drop on both tasks with respect to bit accuracy and image quality. We provide visualization results in the following content to prove images generated by Warfare are still visually close to the given image under a longer embedding length. More importantly, Warfare is time-efficient compared to diffusion model methods. The results are in the supplementary materials.

Few-Shot Generalization. In real-world applications, large companies can assign a unique watermark for every account or change watermarks periodically. Therefore, it is important to study the few-shot power of Warfare, i.e., fine-tuning Warfare with several new data with an unseen watermark to achieve outstanding watermark removal or forging abilities for the unseen watermark. In our experiments, we mainly consider embedding a 32-bit string into clean images. Then, we fine-tune the model in Table 3 to fit new unseen watermarks. In Table 5, we present the results under 10, 50, and 100 training data for watermark removal and forging. The results indicate that the watermark removal task is much easier than the watermark forging task. Furthermore, with more accessible data, both bit accuracy and image quality can be improved. It is worth noticing that, even with limited data, Warfare can successfully remove or forge an unseen watermark and maintain high image quality. The results prove that our proposed method has strong few-shot generalization power to meet practical usage.

Visualization. To better compare the image quality of Warfare with other baselines, we show the visualization results in Figure 2. Specifically, both DM_s and DM_l will change the semantic information in inputs. Warfare can keep the image details in the watermark removal and forging

tasks. Furthermore, when comparing the differences between clean and watermarked images, we find that Warfare can produce a similar residual as the watermark embedding model, which means that Warfare can learn the embedding information during the training process. Note that the generated images by Warfare will be improved with bigger model structures and training data. Because our principal aim is to prove the effectiveness of our method, the generator we use is quite simple. The structure of our generator is several cascaded Residual blocks, which can be replaced with more advanced structures, such as Style-GAN [25]. Therefore, we believe that it will be easy to further improve the image quality. More results can be found in the supplementary materials.

5.4. Results on Prior Manners

We focus on prior methods, i.e., directly embedding watermarks into generative models. We follow the previous methods [15] and [53] to embed a secret bit string into a WGANdiv and an EDM as a watermark, respectively. Therefore, all generated images contain a pre-defined watermark, but we cannot have the corresponding clean images. That is to say, we cannot obtain the PSNR, SSIM, and CLIP scores as previously. So, we only evaluate the FID and the bit accuracy in our experiments. Specifically, we train the WGAN-div with 100,000 watermarked images randomly selected from the training set of CelebA. We directly use the models provided by [53], which are trained on FFHO embedded with a 64-bit string. For Warfare, we use the WGAN-div and EDM to generate 10,000 samples as the accessible data. In Table 6, we show the results of different attacks to remove or forge the watermark. First, we find that embedding a watermark in the generative model will cause the generated images to have a different distribution from the clean images, making the FID extremely high. Second, EDM can generate highquality images even under watermarking, causing a lower



Figure 2. The first column is clean images. The second is watermarked images. The third is the output of DM_l . The fourth is the output of DM_s . The fifth is the output of $\mathrm{Warfare}$. The sixth is the difference between the first and second columns. The seventh is the difference between the first and fourth columns. The ninth is the difference between the first and fifth columns. The tenth is the difference between the second and fifth columns.

			WGA	N-div			EDM						
Methods	Origi	inal	Watermark Remove		Watermar	k Forge	Origi	nal	Watermar	k Remove	Watermar	k Forge	
	Bit Acc	FID	Bit Acc↓	FID↓	Bit Acc↑	FID↓	Bit Acc	FID	Bit Acc↓	FID↓	Bit Acc↑	FID ↓	
CenterCrop			58.05%	-	48.25%	-			61.31%	-	50.23%	-	
GaussianNoise			99.09%	100.65	52.24%	41.58			82.20%	56.43	50.50%	50.98	
GaussianBlur			99.59%	56.83	52.04%	22.85			64.10%	40.04	51.42%	36.49	
JPEG			98.43%	64.09	52.30%	15.12			52.90%	26.81	49.89%	21.21	
Brightness			99.65%	56.99	52.14%	0.63			99.43%	8.30	51.15%	0.65	
Gamma	99.66%	60.20	99.66%	60.59	52.25%	0.47	99.99%	8.68	99.93%	9.12	51.16%	0.37	
Hue			99.55%	63.70	52.17%	1.83			99.86%	8.96	50.92%	2.16	
Contrast			99.66%	57.47	52.27%	0.32			99.79%	50.98	51.11%	0.39	
DM_s			67.12%	100.93	49.17%	68.79	6		51.03%	78.08	51.14%	79.75	
DM_l			47.16%	117.80	46.20%	83.36			51.69%	58.39	51.31%	60.00	
Warfare			52.12%	69.88	95.72%	5.84			64.56%	19.58	90.75%	5.98	

Table 6. Results of removing and forging content watermarks from the WGAN-div and EDM.



Figure 3. Clean images and corresponding outputs from Warfare. The top two rows are clean images.

FID. However, we find that the embedded watermark by [53] is less robust, which can be removed by blurring and JPEG compression. It could be because they made some trade-off between image quality and robustness. For both, Warfare can successfully remove and forge the specific watermark in the generated images and maintain the same image quality as the generative model. The visualization results can be found in the supplementary materials.

Overall, in our experiments, Warfare can pass the watermark verification process for the watermarking forging attack. And Warfare will make the image fail to pass the watermark verification process for the watermark removal attack. Therefore, Warfare is a practical threat for both post hoc methods and prior methods.

5.5. Large-Resolution and Complex Images

To better show the practical usage on large and complex images, in Figure 3, we compare the images from LSUN [49] before and after Warfare, in which our target is to forge a specific watermark. It is difficult for human eyes to determine which clean images are, which shows that Warfare can maintain impressive image quality even for complex and large-resolution images. Clearly, Warfare is still effective for large-resolution and complex images. More analysis can be found in the supplementary materials.

6. Limitations and Conclusions

In this paper, we consider a practical threat to AIGC protection and regulation schemes, which are based on the state-of-the-art **robust and invisible** watermarking technologies. We introduce Warfare, a unified attack framework to effectively remove or forge watermarks over AIGC while maintaining good image quality. With Warfare, the adversary only requires watermarked images without their corresponding clean ones, making it a real-world threat. Through comprehensive experiments, we prove that Warfare has strong few-shot generalization abilities to fit unseen watermarks, which makes it more powerful. Furthermore, we show that Warfare can easily replace a watermark in the collected data with another new one, in the supplementary materials.

We discuss the potential usage of Warfare for larger-

resolution and more complex images, in real-world scenarios. We believe that further improvement over Warfare is probable with more advanced GAN structures and training strategies. In the supplementary materials, we discuss potential defenses and social impact of our work. Warfare brings both positive and negative impacts on society.

References

- [1] Governments race to regulate ai tools. https://www.reuters.com/technology/governments-efforts-regulate-ai-tools-2023-04-12/.1
- [2] A comprehensive guide to the aigc measures issued by the cac. https://www.lexology.com/library/detail.aspx?g=42ad7be8-76bd-40c8-ae5d-271aaf3710eb.1
- [3] Instagram. https://www.instagram.com/. 2
- [4] Midjourney. https://docs.midjourney.com/. 1, 3
- [5] Best sites to sell ai art make profit from day one. https: //okuha.com/best-sites-to-sell-ai-art/. 1
- [6] Singapore's approach to ai governance. https://www.pdpc.gov.sg/help-and-resources/2020/01/model-ai-governance-framework. 1
- [7] Synthid. https://www.deepmind.com/synthid. 1
- [8] Twitter. https://twitter.com/. 2
- [9] Introducing chatgpt. https://openai.com/blog/ chatgpt. 1, 2
- [10] Martín Arjovsky, Soumith Chintala, and Léon Bottou. Wasserstein GAN. CoRR, abs/1701.07875, 2017. 4
- [11] Clark Barrett, Brad Boyd, Ellie Burzstein, Nicholas Carlini, Brad Chen, Jihye Choi, Amrita Roy Chowdhury, Mihai Christodorescu, Anupam Datta, Soheil Feizi, Kathleen Fisher, Tatsunori Hashimoto, Dan Hendrycks, Somesh Jha, Daniel Kang, Florian Kerschbaum, Eric Mitchell, John Mitchell, Zulfikar Ramzan, Khawaja Shams, Dawn Song, Ankur Taly, and Diyi Yang. Identifying and mitigating the security risks of generative ai. CoRR, abs/2308.14840, 2023.
- [12] P. V. Sai Charan, Hrushikesh Chunduri, P. Mohan Anand, and Sandeep K. Shukla. From Text to MITRE Techniques: Exploring the Malicious Use of Large Language Models for Generating Cyber Attack Payloads. *CoRR*, abs/2305.15336, 2023. 1
- [13] Danni Cheng, Xiang Li, Weihong Li, Chan Lu, Fake Li, Hua Zhao, and Wei-Shi Zheng. Large-scale visible watermark detection and removal with deep convolutional networks. In *Proc. of the PRCV*, pages 27–40, 2018. 2
- [14] Yingqian Cui, Jie Ren, Han Xu, Pengfei He, Hui Liu, Lichao Sun, and Jiliang Tang. Diffusionshield: A watermark for copyright protection against generative diffusion models. *CoRR*, abs/2306.04642, 2023. 2, 3
- [15] Jianwei Fei, Zhihua Xia, Benedetta Tondi, and Mauro Barni. Supervised GAN Watermarking for Intellectual Property Protection. In 2022 IEEE International Workshop on Information Forensics and Security (WIFS), pages 1–6, 2022. 2, 3, 5, 7
- [16] Pierre Fernandez, Alexandre Sablayrolles, Teddy Furon, Hervé Jégou, and Matthijs Douze. Watermarking images in self-supervised latent spaces. In *Proc. of the ICASSP*, pages 3054–3058, 2022. 5

- [17] Pierre Fernandez, Guillaume Couairon, Herv'e J'egou, Matthijs Douze, and T. Furon. The Stable Signature: Rooting Watermarks in Latent Diffusion Models. *CoRR*, abs/2303.15435, 2023. 1, 2, 3
- [18] Bin Guo, Yasan Ding, Yueheng Sun, Shuai Ma, Ke Li, and Zhiwen Yu. The mass, fake news, and cognition security. Frontiers in Computer Science, 15(3):153806, 2021.
- [19] Julian Hazell. Large Language Models Can Be Used To Effectively Scale Spear Phishing Campaigns. CoRR, abs/2305.06972, 2023. 1
- [20] Kaiming He, Xiangyu Zhang, Shaoqing Ren, and Jian Sun. Deep Residual Learning for Image Recognition. In *Proc. of the CVPR*, pages 770–778, 2016. 10
- [21] Martin Heusel, Hubert Ramsauer, Thomas Unterthiner, Bernhard Nessler, and Sepp Hochreiter. Gans trained by a two time-scale update rule converge to a local nash equilibrium. In *Proc. of the NeurIPS*, pages 6626–6637, 2017. 6
- [22] Jonathan Ho, Ajay Jain, and Pieter Abbeel. Denoising Diffusion Probabilistic Models. In *Proc. of the NeurIPS*, 2020.
 2
- [23] Jonathan Ho, Tim Salimans, Alexey A. Gritsenko, William Chan, Mohammad Norouzi, and David J. Fleet. Video Diffusion Models. In *Proc. of the NeurIPS*, 2022. 2
- [24] Alain Horé and Djemel Ziou. Image quality metrics: Psnr vs. ssim. In *Proc. of the ICPR*, pages 2366–2369, 2010. 6
- [25] Tero Karras, Samuli Laine, and Timo Aila. A style-based generator architecture for generative adversarial networks. In *Proc. of the CVPR*, pages 4401–4410, 2019. 7, 10
- [26] Tero Karras, Miika Aittala, Timo Aila, and Samuli Laine. Elucidating the design space of diffusion-based generative models. In *Proc. of the NeurIPS*, 2022. 5
- [27] John Kirchenbauer, Jonas Geiping, Yuxin Wen, Manli Shu, Khalid Saifullah, Kezhi Kong, Kasun Fernando, Aniruddha Saha, Micah Goldblum, and Tom Goldstein. On the Reliability of Watermarks for Large Language Models. *CoRR*, abs/2306.04634, 2023. 1
- [28] Zhifeng Kong, Wei Ping, Jiaji Huang, Kexin Zhao, and Bryan Catanzaro. DiffWave: A Versatile Diffusion Model for Audio Synthesis. In *Proc. of the ICLR*, 2021. 2
- [29] Thanh Van Le, Hao Phung, Thuan Hoang Nguyen, Quan Dao, Ngoc Tran, and Anh Tran. Anti-DreamBooth: Protecting users from personalized text-to-image synthesis. *CoRR*, abs/2303.15433, 2023. 1
- [30] Xinyu Li. Diffwa: Diffusion models for watermark attack. CoRR, abs/2306.12790, 2023. 2, 3, 5
- [31] Jing Liang, Li Niu, Fengjun Guo, Teng Long, and Liqing Zhang. Visible watermark removal via self-calibrated localization and background refinement. In *Proc. of the MM*, pages 4426–4434, 2021. 2, 3
- [32] Yang Liu, Zhen Zhu, and Xiang Bai. Wdnet: Watermark-decomposition network for visible watermark removal. In *Proc. of the WACV*, pages 3684–3692, 2021. 2
- [33] Yi Liu, Gelei Deng, Yuekang Li, Kailong Wang, Tianwei Zhang, Yepang Liu, Haoyu Wang, Yan Zheng, and Yang Liu. Prompt Injection attack against LLM-integrated Applications. *CoRR*, abs/2306.05499, 2023. 1

- [34] Yugeng Liu, Zheng Li, Michael Backes, Yun Shen, and Yang Zhang. Watermarking Diffusion Model. *CoRR*, abs/2305.12502, 2023. 1, 3
- [35] Ziwei Liu, Ping Luo, Xiaogang Wang, and Xiaoou Tang. Deep Learning Face Attributes in the Wild. In *Proc. of the ICCV*, 2015.
- [36] Seung-Hun Nam, In-Jae Yu, Seung-Min Mun, Daesik Kim, and Wonhyuk Ahn. WAN: watermarking attack network. In *Proc. of the BMVC*, page 420, 2021. 2, 3
- [37] Weili Nie, Brandon Guo, Yujia Huang, Chaowei Xiao, Arash Vahdat, and Animashree Anandkumar. Diffusion models for adversarial purification. In *Proc. of the ICML*, pages 16805– 16827, 2022. 5
- [38] Xiangyu Qi, Kaixuan Huang, Ashwinee Panda, Mengdi Wang, and Prateek Mittal. Visual Adversarial Examples Jailbreak Large Language Models. CoRR, abs/2306.13213, 2023. 1
- [39] Alec Radford, Jong Wook Kim, Chris Hallacy, Aditya Ramesh, Gabriel Goh, Sandhini Agarwal, Girish Sastry, Amanda Askell, Pamela Mishkin, Jack Clark, Gretchen Krueger, and Ilya Sutskever. Learning transferable visual models from natural language supervision. In *Proc. of the ICML*, pages 8748–8763, 2021. 6
- [40] Robin Rombach, Andreas Blattmann, Dominik Lorenz, Patrick Esser, and Björn Ommer. High-Resolution Image Synthesis with Latent Diffusion Models. In *Proc. of the* CVPR, pages 10674–10685, 2022. 1, 2
- [41] Hadi Salman, Alaa Khaddaj, Guillaume Leclerc, Andrew Ilyas, and Aleksander Madry. Raising the Cost of Malicious AI-Powered Image Editing. CoRR, abs/2302.06588, 2023.
- [42] Matthew Tancik, Ben Mildenhall, and Ren Ng. Stegastamp: Invisible hyperlinks in physical photographs. In *Proc. of the CVPR*, pages 2114–2123, 2020. 1, 2, 5
- [43] Hugo Touvron, Thibaut Lavril, Gautier Izacard, Xavier Martinet, Marie-Anne Lachaux, Timothée Lacroix, Baptiste Rozière, Naman Goyal, Eric Hambro, Faisal Azhar, Aurélien Rodriguez, Armand Joulin, Edouard Grave, and Guillaume Lample. LLaMA: Open and Efficient Foundation Language Models. CoRR, abs/2302.13971, 2023. 1, 2
- [44] Dmitry Ulyanov, Andrea Vedaldi, and Victor S. Lempitsky. Deep image prior. In *Proc. of the CVPR*, pages 9446–9454, 2018. 2, 3
- [45] Chunpeng Wang, Qixian Hao, Shujiang Xu, Bin Ma, Zhiqiu Xia, Qi Li, Jian Li, and Yun-Qing Shi. RD-IWAN: residual dense based imperceptible watermark attack network. *IEEE Transactions on Circuits and Systems for Video Technology*, 32(11):7460–7472, 2022. 2, 3
- [46] Alexander Wei, Nika Haghtalab, and Jacob Steinhardt. Jail-broken: How Does LLM Safety Training Fail? CoRR, abs/2307.02483, 2023. 1
- [47] Yuxin Wen, John Kirchenbauer, Jonas Geiping, and Tom Goldstein. Tree-ring watermarks: Fingerprints for diffusion images that are invisible and robust. *CoRR*, abs/2305.20030, 2023, 2, 3
- [48] Jiqing Wu, Zhiwu Huang, Janine Thoma, Dinesh Acharya, and Luc Van Gool. Wasserstein divergence for gans. In *Proc. of the ECCV*, pages 673–688, 2018. 5

- [49] Fisher Yu, Yinda Zhang, Shuran Song, Ari Seff, and Jianxiong Xiao. LSUN: construction of a large-scale image dataset using deep learning with humans in the loop. *CoRR*, abs/1506.03365, 2015. 5, 8, 11, 12
- [50] Kevin Alex Zhang, Lei Xu, Alfredo Cuesta-Infante, and Kalyan Veeramachaneni. Robust invisible video watermarking with attention. *CoRR*, abs/1909.01285, 2019. 5
- [51] Richard Zhang, Phillip Isola, Alexei A. Efros, Eli Shechtman, and Oliver Wang. The Unreasonable Effectiveness of Deep Features as a Perceptual Metric. In *Proc. of the CVPR*, pages 586–595, 2018. 4
- [52] Xuandong Zhao, Kexun Zhang, Zihao Su, Saastha Vasan, Ilya Grishchenko, Christopher Kruegel, Giovanni Vigna, Yu-Xiang Wang, and Lei Li. Invisible image watermarks are provably removable using generative ai. *CoRR*, abs/2306.01953, 2023. 2, 3, 5
- [53] Yunqing Zhao, Tianyu Pang, Chao Du, Xiao Yang, Ngai-Man Cheung, and Min Lin. A recipe for watermarking diffusion models. *CoRR*, abs/2303.10137, 2023. 1, 2, 3, 5, 7, 8
- [54] Jun-Yan Zhu, Taesung Park, Phillip Isola, and Alexei A. Efros. Unpaired image-to-image translation using cycle-consistent adversarial networks. In *Proc. of the ICCV*, pages 2242–2251, 2017. 10
- [55] Jiren Zhu, Russell Kaplan, Justin Johnson, and Li Fei-Fei. Hidden: Hiding data with deep networks. In *Proc. of the ECCV*, pages 682–697, 2018. 1, 2

A. Experiment Settings

Model Structures. For CIFAR-10 and CelebA, we choose different architectures for generators and discriminators to stabilize the training process. Specifically, when training models on CIFAR-10, we use the ResNet-based generator architecture [54] with 6 blocks. As the CelebA images have higher resolution, we use the ResNet-based generator architecture [54] with 9 blocks. For the discriminators, we use a simple model containing 4 convolutional layers for CIFAR-10. And for CelebA, a simple discriminator cannot promise a stable training process. Therefore, we use a ResNet-18 [20]. To improve the quality of generated images, we follow the residual training manner, that is, the output from the generators will be added to the original input.

Hyperparameters. We use different hyperparameters for CIFAR-10 and CelebA, respectively. When training models on CIFAR-10, we use RMSprop as the optimizer for both the generator and the discriminator. The learning rate is 0.0001, and the batch size is 32. We set $w_{\mathcal{D}} = 10$, and the total number of training epochs is 1,000. We update the generator's parameters after 5 times of updating of the discriminator's parameters. For CelebA, we adopt Adam as our model optimizer. The learning rate is 0.003, and the batch size is 16. We replace the discriminator loss with the one from StyleGAN [25] with $w_{\mathcal{D}} = 5$, and the total number of training epochs is 1,000. We update the generator's parameters after updating the discriminator's

parameters. We present $w_{\mathcal{G}}$ and w_x in Table 7 used in our experiments. We choose the best model based on the image quality.

Baseline Settings. For image transformation methods, we mainly adopt torchvision to implement attacks. To adjust brightness, contrast, and gamma, the changing range is randomly selected from 0.5 to 1.5. To adjust the hue, the range is randomly selected from -0.1 to 0.1. For centercropping, we randomly select the resolution from 32 to 64. For the Gaussian blurring, we randomly choose the Gaussian kernel size from 3, 5, and 7. For adding Gaussian noise, we randomly choose σ from 0.0 to 0.1. For JPEG compression, we randomly selected the compression ratio from 50 to 100. When evaluating the results of image transformation methods, we run multiple times and use the average results. For diffusion methods DM_l , we set the sample step as 30 and the noise scale as 150. For diffusion methods DM_s , we set the sample step as 200 and the noise scale as 10. Specifically, we use DM_l in the second step of Warfare. Considering using diffusion models to generate images is very time-consuming, we randomly select 1,000 images from the test set to obtain the results for diffusion models.

Embedded Bits. In Table 8, we list the bit strings embedded in the images in our experiments.

B. Select a Correct Checkpoint

It is important to choose the correct checkpoint because it is closely associated with the attack performance. However, when the adversary does not have any information about the watermarking scheme, it is unavailable to determine the best checkpoint with Bit Acc as metrics. However, after plotting the bit accuracy in Figure 4, we find that the performances of different checkpoints in the later period are close and acceptable for a successful attack under the Bit ACC metrics. Therefore, we choose the best checkpoint from the later training period based on the image quality metrics, including the FID, SSIM, and PSNR, in our experiments. It is to say, our selection strategy does not violate the threat model, where the adversary can only obtain watermarked images.

C. Diffusion Models for Watermark Removal

In our experiments, we find that the pre-trained diffusion models will not promise a similar output as the input image without the guidance on CelebA. However, when we evaluate the diffusion models on another dataset, LSUN-bedroom [49], we find that even under a very large noise scale, the output of the diffusion model is very close to the input image, and the watermark has been successfully removed. The visualization results can be found in Figure 5, where we use 30 sample steps and 150 noise scales for DM_l and use 200 sample steps and 10 noise scales for DM_s , which are the same as the settings on CelebA. The numerical results

in Table 9 prove that the diffusion model can maintain high image quality under large inserted noise.

We think the performance differences on CelebA and LSUN are related to the resolution and image distribution. Specifically, images in CelebA are 64 * 64 and only contain human faces. The diversity of faces is not too high. However, images in LSUN are 256 * 256 and have different decoration styles, illumination, and perspective, which means the diversity of bedrooms is very high. Therefore, transforming an image into another image in LSUN is more challenging than doing that in CelebA. This could be the reason that diffusion models cannot produce an output similar to that of CelebA. This limitation is critical for an attack based on diffusion models. Therefore, we appeal to comprehensively evaluate the performance of the watermark removal task for various datasets.

D. Time Cost vs Diffusion Models

To compare the time cost for generating one image with a given one, we record the total time cost for 1,000 images on one A100. The batch size is fixed to 128. For DM_l , the total time cost is 5,231.72 seconds. For DM_s , the total time cost is 2325.01 seconds. For $\mathrm{Warfare}$, the total time cost is **0.46** seconds. Therefore, our method is very fast and efficient.

E. Replace a Watermark with New One

We further consider another attack scenario, where the adversary wants to replace the watermark in the collected images with one specific watermark used by other users or companies. In this case, the adversary first trains a generator G_r to remove the watermark in the collected image x. Then, the adversary trains another generator G_f to forge the specific watermark. Finally, to replace the watermark in x with the new watermark, the adversary only needs to obtain $x' = G_f(G_r(x))$. We evaluate the performance of Warfare in this scenario on CelebA. Specifically, G_r is the generator in our few-shot experiment. And G_f is the generator in our CelebA 32bit experiment. It is to say that the existing watermark in the collected images is "11100011101010101000010000001011", and the adversary wants to replace it with "1000100010001 0001000100010001000". The details can be found in our main paper. As for the results, we calculate PSNR, SSIM, CLIP score, and FID between x' and clean images. And we also compute the bit accuracy of x' for the new watermark. The FID is 18.67. The PSNR is 24.97. The SSIM is 0.90. The CLIP score is 0.92. And the bit accuracy is 98.86%. The results prove that Warfare can easily replace an existing watermark in the images with a new watermark.

Experiment	Water	mark Remove	Water	mark Forge
Experiment	$w_{\mathcal{G}}$	w_x	$w_{\mathcal{G}}$	w_x
CIFAR-10 4bit	500	10	500	5
CIFAR-10 8bit	800	15	500	10
CIFAR-10 16bit	500	40	150	40
CIFAR-10 32bit	100	40	100	40
CIFAR-10 5000 data	800	15	500	10
CIFAR-10 10000 data	800	15	600	20
CIFAR-10 15000 data	500	15	500	10
CIFAR-10 20000 data	800	15	500	15
CIFAR-10 25000 data	800	15	500	10
CelebA 32bit	10	120	1	10
CelebA 48bit	10	200	1	10
Few-Shot 10 Images	10	200	1	10
Few-Shot 50 Images	10	200	1	10
Few-Shot 100 Images	10	200	1	10
WGAN-div	10	120	1	10
EDM	1	10	100	1

Table 7. Hyperparameter settings in our experiments for watermark removal and watermark forging.

Experiment	Bit String
CIFAR-10 4bit	1000
CIFAR-10 8bit	10001000
CIFAR-10 16bit	1000100010001
CIFAR-10 32bit	10001000100010001000100010001000
CelebA 32bit	10001000100010001000100010001000
CelebA 48bit	100010001000100010001000100010001000100010001000
Few-Shot	1110001110101010100001000001011
WGAN-div	10001000100010001000100010001000
EDM	0100010001000010111010111111111100111010

Table 8. Selected bit strings in our experiments.

F. Other Visualization Results

In this section, we show the other visualization results in our experiments. In Figure 6, we present the visualization results for the few-shot experiments. The results indicate that with more training samples, image quality can be improved. And, even with a few samples, Warfare can learn the embedding pattern. In Figure 7, we show the visualization results of WGAN-div and EDM, respectively. The attack goal is to forge a specific watermark. The results indicate that Warfare can generate images with the specific watermark, keeping high quality simultaneously.

G. Large-Resolution and Complex Images

We focus on CelebA in our main paper, which contains human faces in a resolution of 64 * 64. In this part, we illustrate the results of our method on larger resolution and more complex images. To evaluate our method on such images, LSUN-bedroom [49] is a good choice, in which the image

resolution is 256 * 256. Similarly to the CelebA experiment settings, we randomly select 10,000 images for Warfare, and the bit length is 32. As watermark removal is easy to do with only diffusion models, forging is more challenging and critical. Therefore, we aim to forge a specific watermark on the clean inputs.

In Figure 8, we illustrate the bit accuracy during the training stage of Warfare. Although accuracy increases with increasing training steps, we find that it is difficult to achieve accuracy over 80%. If we increase the number of training steps, the accuracy will be stable around 75%. While Warfare is still effective for large-resolution and complex images, we think its ability is constrained, due to the limited training data and a small generator structure. Our future work will be to improve its effectiveness for more complex data.

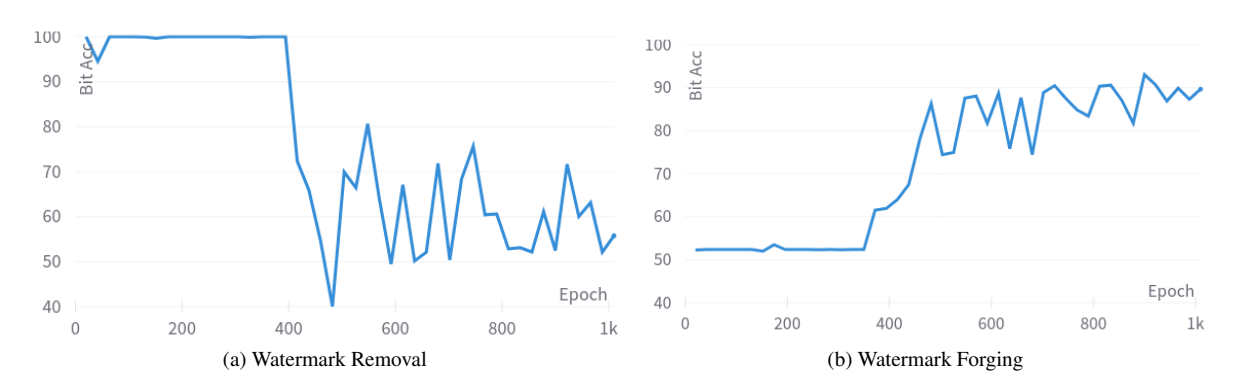


Figure 4. Bit Acc for different tasks during the training stage on CelebA.

Diffusion Me (bit length		Original			Watermark Remove						
Sample Step	Noise Scale	Bit Acc	FID	PSNR	SSIM	CLIP	Bit Acc	FID	PSNR	SSIM	CLIP
30	150						51.81%	75.52	20.15	0.58	0.88
50	150						51.50%	84.14	18.92	0.55	0.86
100	150	100.00%	10.67	7 39.49 0.98 0.99 50.47% 95.27 56.16% 73.01 53.03% 98.00 53.81% 108.71	16.69	0.49	0.83				
200	10	100.00%	10.67		0.98	0.99	56.16%	73.01	22.11	0.72	0.84
200	30						53.03%	98.00	19.37	0.59	0.80
200	50						53.81%	108.71	17.63	0.52	0.78

Table 9. Numerical results of watermark removal with diffusion models under different noise scales and sample steps.

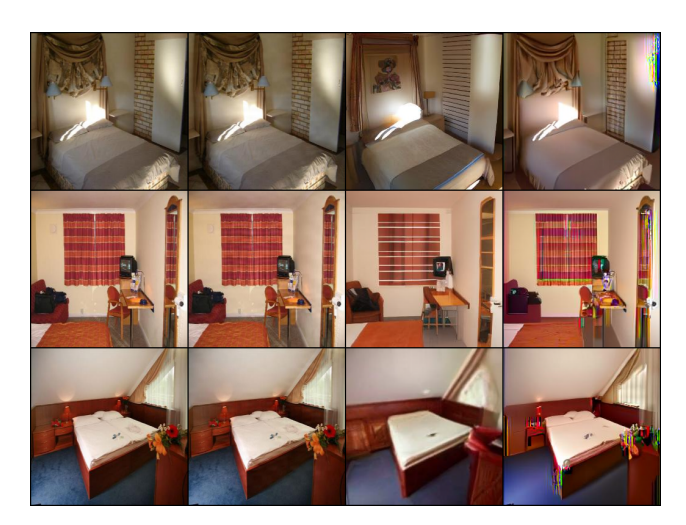
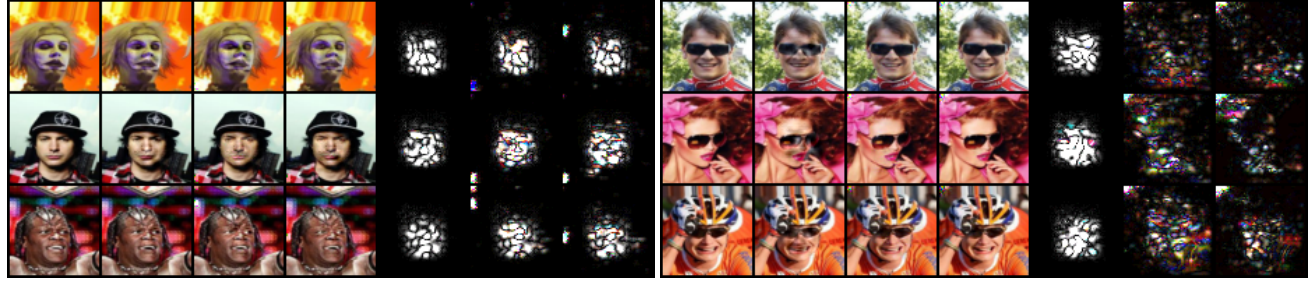


Figure 5. The first column is clean images. The second is water-marked images. The third is the output of DM_l . The fourth is the output of DM_s .

H. Potential Defenses for Service Providers

Although Warfare is an effective method for removing or forging a specific watermark in images, there are some possible defense methods against our attack. First, large companies can assign a group of watermarks to an account to identify the identity. When adding watermarks to images, the watermark can be randomly selected from the group of watermarks, which can hinder the adversary from obtaining

images containing the same watermark. However, such a method requires a longer length of embedded watermarks to meet the population of users, which will decrease image quality because embedding a longer watermark will damage the image. We provide a case study to verify such a defense. In our implementation, we choose to use two bit strings for one user, i.e., m_1 is '1000100010001000100010001000' and m_2 is '1110001110101010100001000001011'. Note that the Hamming Distance between m_1 and m_2 is 12, which means that there are 12 bits in m_1 and m_2 are different. We assume that m_1 and m_2 will be used with equal probability. Therefore, half of the collected data contain m_1 and others contain m_2 . We evaluate Warfare on this collected dataset. For the watermark removal attack, the bit accuracy for m_1 after Warfare is 71.04%. And the bit accuracy for m_2 after Warfare is 64.87%. Note that the ideal bit accuracy after the removal attack is (32 - 12)/32 * 100% = 62.50%. Therefore, our method can maintain the attack success rate to some degree. For the watermark forging attack, the bit accuracy for m_1 after Warfare is 87.53%. And the bit accuracy for m_2 after Warfare is 69.21%. We notice that the ideal bit accuracy for the forging attack is (32 - 12 + 6)/32 * 100% = 81.25%, which means that 26 bits can be correctly recognized. The results indicate that the generator does not equally learn m_1 and m_2 . We think it is because of the randomness in the training process. On the other hand, the results indicate that such a defense can improve the robustness of the watermark. However, we find



(a) Watermark Removal (b) Watermark Forging

Figure 6. The first column is clean images. The second is watermarked images. The third is the output of Warfare under the 50-sample setting in the few-shot experiment. The fourth is the output of Warfare under the 100-sample setting in the few-shot experiment. The fifth is the difference between the first and second columns. The sixth is the difference between the first and third columns. The seventh is the difference between the first and fourth columns.

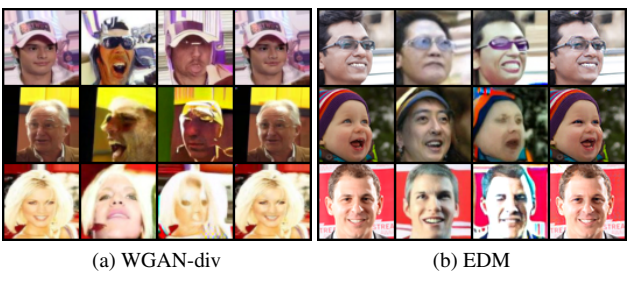


Figure 7. Visualization results for prior watermarking methods. The first column is clean images. The second is the output of DM_t . The third is the output of DM_s . The fourth is the output of Warfare.

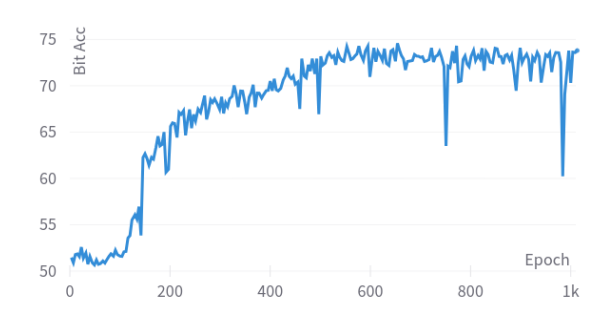


Figure 8. Bit Acc with training epoch increasing.

Warfare can still remove or forge one of the two watermarks. This means that such a defense can only alleviate security problems instead of addressing them thoroughly.

Another defense is to design a more robust watermarking scheme, which can defend against removal attacks from diffusion models. Because Warfare requires diffusion models to remove the watermarks. The two methods mentioned above have the potential to defend against Warfare but have different shortcomings, such as decreasing image quality, requiring a newly designed coding scheme, and requiring a newly designed robust watermarking scheme. Therefore, Warfare will be a threat for future years.

I. Social Impact

We think that the proposed Warfare will cause some malicious users to freely make the AIGC for commercial use. Furthermore, malicious users could frame their users by spreading illegal AIGC with forged watermarks. We think they are some negative impacts from our research. But, on the other hand, our work will encourage others to explore a more robust and reliable watermark for AIGC, which is a positive impact on society.